

BLACK HOLE SHADOW DRIFT AND PHOTON RING FREQUENCY DRIFT

EMMANUEL FRION

University of Helsinki, Department of Physics and Helsinki Institute of Physics,
P.O. Box 64, FIN-00014 University of Helsinki, Finland

LEONARDO GIANI

The University of Queensland, School of Mathematics and Physics,
QLD 4072, Australia

TAYS MIRANDA

University of Helsinki, Department of Physics and Helsinki Institute of Physics,
P.O. Box 64, FIN-00014 University of Helsinki, Finland
Department of Physics, University of Jyväskylä, P.O. Box 35, FIN-40014 Finland

Abstract

The apparent angular size of the shadow of a black hole in an expanding Universe is redshift-dependent. Since cosmological redshifts change with time - known as the redshift drift - all redshift-dependent quantities acquire a time-dependence, and *a fortiori* so do black hole shadows. We find a mathematical description of the black hole shadow drift and show that the amplitude of this effect is of order 10^{-16} per day for M87*. While this effect is small, we argue that its non-detection can be used as a novel probe of the equivalence principle and derive a constraint of $|\dot{G}/G| \leq 10^{-3} - 10^{-4}$ per year. The effect of redshift drift on the visibility amplitude and frequency of the universal interferometric signatures of photon rings is also discussed, which we show to be very similar to the shadow drift. This is of particular interest for future experiments involving spectroscopic and interferometric techniques, which could make observations of photon rings and their frequency drifts viable.

1. INTRODUCTION

Redshift is an omnipresent Doppler-effect-related quantity, used in cosmology to build meaningful spatial and temporal distances. In 1962, Sandage and McVittie [1, 2] showed that the redshift is in fact a dynamical quantity, now labeled as redshift drift. A redshift drift driven by the expansion of the Universe is called a cosmological drift¹, with the interesting consequence of turning redshift-dependent quantities into time-dependent ones. The cosmological drift depends on the Hubble rate $H(z)$, and is expected to be very small at low redshift z , with a redshift change of the order of 10^{-10} per year. However, it applies to every object in the Universe, which makes all of them possible probes of the drift, and collaborations such as the Extremely Large Telescope, the Square-Kilometer Array or the Vera C. Rubin Observatory will provide means of its detection. Optimistic estimates show that these facilities could reach a precision of 10^{-10} , for example with monitoring programs of 1000 hours of exposure with a 40-meter telescope [4]. For this reason, cosmology with redshift drifts is an active field of research [5–18], which we advance further with this work, in which we investigate how the cosmological drift would affect the image from black hole shadows and interferometric signatures from black holes' photon rings.

Black holes were first predicted over a century ago, yet the first direct image of a black hole was reconstructed only very recently by the Event Horizon Telescope (EHT) collaboration [19–25]. The direct detection of the shadow of M87*, the supermassive black hole at the centre of the galaxy Messier 87, suggests we will soon be able to obtain black hole parameters such as their mass, spin and charge in a systematic way. Black holes shadows and photons rings are observables that can be used to infer these parameters [26–34], and are particularly interesting to precisely constrain gravity in the strong-field regime [35–40]. In fact, black hole shadows could potentially be used as standard rulers to infer the present day value of the Hubble parameter H_0 once that the mass of the black hole has been inferred independently [41]. These aspects (and more) about black hole shadows are covered in the recent review [42].

The shadow of a black hole is surrounded by a bright area, clearly visible in the image resolved by the EHT. This image was obtained using a baseline with roughly the same size of the diameter of the Earth. As a consequence, most of the luminosity comes from astrophysical processes taking place in the disk and jet of M87*. To distinguish the luminosity emitted by the rings, much longer baselines are required [43, 44]. While the luminosity flux of photon rings is exponentially decreasing with each orbit, the signal is dominated by periodic universal interferometric signatures for baselines greater than approximately $20 G\lambda$ ² (see figure 4 of [43]), with the period inversely proportional to the diameter of the ring. We show in this work that cosmological expansion affects both the angular size of black hole shadows and the periodic signal in the same fashion. Furthermore, we discuss the possibility of using the non-detection of a black hole shadow drift as another probe of the equivalence principle.

emmanuel.frion@helsinki.fi
uqlgiani@uq.edu.au
tays.miranda@helsinki.fi

¹ Other contributions from peculiar velocities and inhomogeneities exist, and are discussed in [3].

² Baselines are often given in units of wavelengths. This is because the telescope resolution (in radians) is obtained through the relation $R = \lambda/u$, with u the baseline. Therefore, when u is proportional to the wavelength, the resolution is simply $R = 1/u$.

2. BLACK HOLE SHADOW DRIFT

2.1. Schwarzschild black hole in an expanding universe

The McVittie metric [45] is a hybrid solution recovering the Schwarzschild metric near the black hole and the flat Friedmann-Lemaître-Robertson-Walker (FLRW) far away from it. Therefore, when the metric is well-defined, it describes a spherically symmetric black hole in an expanding Universe. Its line element is usually written as

$$ds^2 = - \left(\frac{1 - \mu}{1 + \mu} \right)^2 c^2 dt^2 + (1 + \mu)^4 a^2(t) (dl^2 + l^2 d\Omega^2) , \quad (1)$$

with

$$\mu := \frac{m}{2a(t)l} . \quad (2)$$

In this definition, l is the radial comoving distance, $a(t)$ is the scale factor characterising the expansion of the Universe, and $m = GM/c^2$, with M the mass of the black hole. For an observer near the black hole, the scale factor is nearly constant and evaluated at $t = t_0$, which allows to recover the Schwarzschild metric with the change of variable

$$R = r \left(1 + \frac{2m}{r} \right)^2 , \quad (3)$$

and the definition $r := a(t_0)l$. The position of the observer at time t_0 is denoted R_O in these coordinates, and t_0 corresponds to the present time.

An approximate solution for black hole shadows in a McVittie spacetime has been found as a composite solution by employing the technique of matching solutions for the Einstein equations [46]:

$$\alpha_{\text{appr}}(R_O) = \alpha_{\text{schw}}(R_O) + \alpha_{\text{cosm}}(R_O) - \alpha_{\text{overlap}}(R_O) , \quad (4)$$

where the three pieces on the right side of the equation are respectively the angular diameter of the shadow when observed from near the Schwarzschild black hole, in an intermediate region far from the black hole but in which the cosmological expansion is negligible, and at cosmological scales. These are defined as:

$$\alpha_{\text{schw}}(R_O) = \begin{cases} \pi - \arcsin\left(3\sqrt{3}m\sqrt{1 - 2m/R_O}/R_O\right) & \text{for } 2m \leq R_O \leq 3m \\ \arcsin\left(3\sqrt{3}m\sqrt{1 - 2m/R_O}/R_O\right) & \text{for } R_O \geq 3m \end{cases} \quad (5)$$

$$\alpha_{\text{overlap}}(R_O) = \frac{3\sqrt{3}m}{R_O} \quad \text{for } m \ll R_O \ll c/H_0 \quad (6)$$

$$\alpha_{\text{cosm}}(R_O) = \frac{3\sqrt{3}m}{D_A(z)} \quad \text{otherwise} . \quad (7)$$

The cosmological solution depends on the redshift z , and, in a flat universe, the apparent size for an observer at cosmological distances depends on the angular diameter distance $D_A(z)$ defined by

$$D_A(z) := \frac{c}{1+z} \int_0^z \frac{d\tilde{z}}{H(\tilde{z})} = \frac{1}{1+z} \chi , \quad (8)$$

with χ the comoving distance to the black hole.

The overlap region is well-defined for an observer at a distance much greater than GM/c^2 . The most massive black holes have a mass reaching 10^{41} kg, which corresponds to $z \approx 10^{-14}$. The upper bound was derived assuming that $z \ll 1$ in [46]. However, since cosmological expansion can be neglected only at scales below the scale of galaxy clusters, and remembering that the closest galaxy clusters are situated at a redshift of $z \approx 10^{-3}$, we can assume that the overlap region should lie in the redshift span $10^{-14} \ll z \ll 10^{-3}$.

2.2. Shadow drift

By construction, only the cosmological term (7) of the composite solution is redshift-dependent. For an observer sufficiently far away from the black hole, this very term is the only one relevant. Therefore, any drift in the shadow angular radius is fully contained into the relation (omitting R_O for conciseness)

$$\frac{\dot{\alpha}_{\text{appr}}}{\alpha_{\text{appr}}} = \frac{\dot{\alpha}_{\text{cosm}}}{\alpha_{\text{cosm}}} . \quad (9)$$

The time derivative of α_{cosm} ,

$$\dot{\alpha}_{\text{cosm}} = -3\sqrt{3}m \frac{\dot{z}}{D_A^2(z)} \frac{dD_A}{dz} = -\alpha_{\text{cosm}} \frac{\dot{z}}{D_A(z)} \frac{dD_A}{dz} , \quad (10)$$

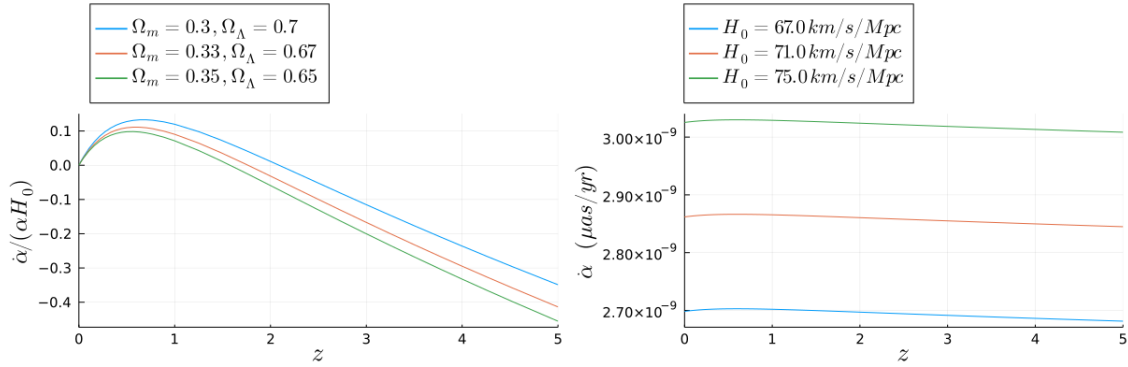


FIGURE 1. Left: Normalised shadow drift as a function of redshift for three sets of matter and dark energy dimensionless densities. At low redshift, the maximum normalised shadow drift is about 0.1 for the three sets, which results in a shadow drift $\dot{\alpha}/\alpha$ of $10^{-14} \text{ day}^{-1}$. Right: Variation of the apparent angular diameter for three different values of the present Hubble rate. We used density values of $\Omega_m = 0.33$ and $\Omega_\Lambda = 0.67$, and assumed an apparent angular diameter $d = 40 \mu\text{as}$.

explicitly depends on the variation of the angular diameter distance (8) with redshift and on the redshift drift \dot{z} . The first quantity is

$$\frac{dD_A}{dz} = -\frac{D_A(z)}{1+z}. \quad (11)$$

Recalling the redshift drift in a FLRW background is [1, 2, 47, 48]

$$\frac{dz}{dt} = H_0(1+z) - H(z), \quad (12)$$

we find the *shadow drift*

$$\frac{\dot{\alpha}}{\alpha} = H_0 - \frac{H(z)}{1+z}, \quad (13)$$

in which we have dropped the subscript in the angular radius for conciseness.

In a flat Λ CDM universe, the Hubble parameter is related to the matter density Ω_{m0} , the radiation density Ω_{r0} and the dark energy density Ω_Λ through

$$H(z) = H_0 \sqrt{\Omega_{m0}(1+z)^3 + \Omega_{r0}(1+z)^4 + \Omega_\Lambda}. \quad (14)$$

In Fig. 1, the left figure shows the shadow drift normalised with H_0 for three sets of dimensionless densities, assuming $\Omega_{r0} = 0$. For each mode, drift effects get much higher with redshift, but the luminosity drops quickly, which makes high-redshift black hole shadows impractical targets in real situations for the current status of observations. Indeed, the observed flux of a source located at redshift z decreases as $(1+z)^2$, while the surface brightness as $(1+z)^4$, so a source at $z = 1$ would see its surface brightness reduced by a factor 16 [49]. We note that there is a small bump at low redshift around $z = 0.5$ where the drift is potentially easier to observe. In the right figure, we display the variation of the angular apparent radius $\dot{\alpha}$. The plot shows that, if given an independent measure of the black hole's mass, we can obtain an independent measure of the Hubble rate today. We have used the density values $\Omega_{m0} = 0.33$, $\Omega_{r0} = 0$ and $\Omega_\Lambda = 0.67$ to obtain this figure.

2.3. Shadow drift of M87*

Let us work out as an example the shadow of the black hole at the centre of the galaxy Messier 87, M87*. The heliocentric radial velocity of M87* is around 1284 km/s [50], with a peculiar velocity of the order of $\sim 10\%$ of the total velocity [51], which we assume to be too small to have a noticeable impact on the shadow drift. We also assume that the contribution from the peculiar accelerations to be negligible, *i.e.*, we suppose the peculiar will not change noticeably. Furthermore, the estimated distance of M87* from us is roughly $z \sim 0.004$ [50]. This distance corresponds to a R_O near the $z \sim 10^{-3}$ upper bound we found for the overlap region defined in the previous section. However, for illustrative purposes, we will assume M87* to be at cosmological distances in order to make a quantitative estimate of the drift effects magnitude. At sufficiently low redshift ($z \ll 1$), we can safely ignore the contribution from radiation in Eq. (14). We use the density values $\Omega_{m0} \simeq 0.31$, $\Omega_\Lambda \simeq 0.67$, and the Hubble rate today $H_0 = 67.8 \text{ km/s/Mpc}$.

The shadow drift is then:

$$\frac{\dot{\alpha}}{\alpha} \approx 2H_0 \times 10^{-3} \approx 3.8 \times 10^{-16} / \text{day}. \quad (15)$$

A tiny variation, which seems far away from the angular resolution the EHT can achieve from Earth.³ Indeed, even for the future Plateau de Bure–South Pole baseline, which should reach a resolution of $15 \mu\text{as}$ at 345 GHz, this seems like an infeasible task.

³ It must be stressed that the EHT is currently capable of resolving objects of size $d \approx 25 \mu\text{as}$, even though through imaging techniques they were able to reach a sensitivity of the order of $\approx 1 \mu\text{as}$ for M87* and SgrA* (see details in EHT IV [19]).

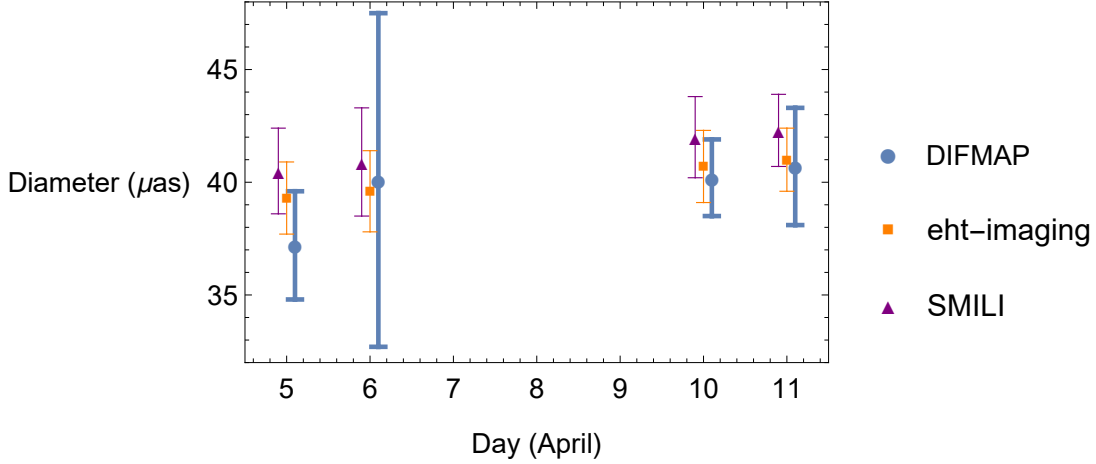


FIGURE 2. The observed diameter of the shadow of M87* measured by the EHT with three different pipelines, DIFMAP, eht-imaging and SMILI, from April 5 to April 11. Data taken from Table 7 of [19].

An Earth–Moon baseline could potentially enhance the resolution by a factor 10, while an Earth–L2 Lagrange point baseline by a factor 100, but does not raise much hope for this detection.

3. SHADOW DRIFT AS A PROBE OF THE EQUIVALENCE PRINCIPLE

We argue in this section that the impossibility of detecting the cosmological shadow drift can be put into good use. Until now, we have considered that only the redshift depends on time, though it would be interesting to let m be a time-dependent quantity as well in the cosmological solution (7). In this case, the three quantities G , M and c could depend on time, but we will keep the speed of light constant in this work.

First, we assume a time-dependent gravitational coupling and a constant mass. Then the right-hand side of the shadow drift (13) has an additional contribution

$$\frac{\dot{\alpha}}{\alpha} = H_0 - \frac{H(z)}{1+z} + \frac{\dot{G}}{G}. \quad (16)$$

Therefore, the non-observation of a drift in the angular shadow within the sensitivity of present experiments provides another probe of the equivalence principle, complementary to other works using black hole shadows to test the equivalence principle [52]. Using the mean values of M87* shadow’s angular diameter reported by the EHT collaboration, which we also plot in Fig. 2, during the period of observations from April 5 to April 11 (see Table 7 in EHT IV [19]), we compute the shadow drift between these two dates for the three different pipelines (DIFMAP, eht-imaging and SMILI) used by the collaboration, summarised in Table 1.

	DIFMAP	eht-imaging	SMILI
$\dot{\alpha}/\alpha$ (10^{-2})	1.6 ± 1.7	0.7 ± 0.9	0.7 ± 0.9

TABLE 1

ESTIMATED VARIATION OF THE ANGULAR SIZE OF M87*’S SHADOW FOR THE THREE PIPELINES USED BY THE EHT COLLABORATION. ALL VALUES ARE GIVEN IN DAY^{-1} .

We can readily see from the table that the non-observation over a period of 6 days implies that $\dot{G}/G \lesssim 10^{-1} - 10^{-2} \text{ day}^{-1}$. Extrapolating over a period of one year would improve the precision to roughly $10^{-3} - 10^{-4} \text{ year}^{-1}$. While this precision is far inferior to other existing probes (the strongest constraint gives $\dot{G}/G \leq 10^{-13} - 10^{-14} \text{ day}^{-1}$, see for example Table 1 from Ref. [53]), we note that the shadow drift only depends on the cosmological model. Therefore, it is an almost model-independent probe of the equivalence principle similar to the one found in [17] in the case of strong lensing.

On the other hand, it must be stressed that a variation of the effective gravitational coupling G is degenerate with a variation of the black hole mass M . Modeling the evolution of a black hole mass through accretion is a cumbersome task, involving many astrophysical processes which ultimately depends on the black hole environment, as discussed for example in Ref. [54]. Consequently, in order to properly employ drift observations of rings and shadows to test the equivalence principle, a reliable accretion model is required. However, assuming that General Relativity is the correct theory of gravitation, for which G is constant, the very same argument shows that the non-observation of a shadow drift can be used to constrain accretion rates \dot{M}/M , since we would now have

$$\frac{\dot{\alpha}}{\alpha} = H_0 - \frac{H(z)}{1+z} + \frac{\dot{M}}{M}. \quad (17)$$

For M87*, which has a mass of roughly $6.5 \times 10^9 M_\odot$ as measured by the EHT collaboration [22], an absence of shadow drift of

order $\dot{\alpha}/\alpha \leq 10^{-4} \text{ year}^{-1}$ implies that the black hole mass has changed less than $10^5 M_\odot$ over a year. ⁴

One way to distinguish between a time dependence of the mass and a time dependence of G is to look at the variation sign of $\dot{\alpha}/\alpha$. Since evaporation is a very slow process, we expect that only accretion would change the mass of the black hole, and therefore $\dot{M}/M > 0$. This implies that if we observe $\dot{\alpha}/\alpha < 0$, the variation of the angular diameter of the shadow can be attributed to a variation in the gravitational coupling, and to the cosmological drift (even if the latter is very small as we discussed in the previous section). To have $\dot{M}/M > 0$, the black hole needs to accrete matter from its surroundings. The maximum efficiency of this process is given by the Eddington rate (see *e.g.* [57])

$$\dot{M}_{Edd} := 0.02 f_{Edd} \frac{M}{10^6 M_\odot} M_\odot \text{yr}^{-1}, \quad (18)$$

where f_{Edd} is the Eddington ratio typically ranging between 10^{-2} and 1 [58]. Note that this formula assumes a radiative efficiency $\eta \approx 0.1$. For M87, the Eddington ratio is expected to be at most $f_{Edd} = 0.03$ [59], resulting in $\dot{M}_{Edd}/M \simeq 6 \times 10^{-10} M_\odot \text{yr}^{-1}$, or, equivalently, in $\dot{M}_{Edd} = 4 M_\odot \text{yr}^{-1}$. The latter estimate implies that the strongest constraint on \dot{G}/G which could be obtained from M87* is of order 10^{-10} yr^{-1} . Alternatively, drifts observations could be used to constrain models of BH accretion, for example to obtain upper bound on the Eddington rate f_{Edd} .

4. RING VISIBILITY AMPLITUDE AND FREQUENCY DRIFTS

We investigate in this section a complementary possibility of observing drift effects with black holes using photon rings, which should be observable for interferometers with baselines u at least greater than $20 G\lambda$ (or, equivalently, for a resolution $1/u$ better than $10 \mu\text{as}$). For such large baselines, the complex visibility $V(u)$ of a Kerr photon ring can be approximated by a damped oscillating function with period $\Delta u = 2/d$, with d the ring diameter [43]. As argued by the authors of [43], all rings are almost circular, independently of the black hole spin and inclination, so we adopt in this section a perfectly circular photon ring model to study the effect of cosmological expansion on the ring diameter. Since the photon ring properties in Schwarzschild do not differ appreciably from Kerr black hole photon rings [60], we assume the conclusions drawn by Johnson et al in [43] hold for a Schwarzschild black hole. For simplicity, we suppose further that all rings are infinitesimally thin and uniform. In this case, the complex visibility is given by a Bessel function of the first kind, $V(u) = J_0(\pi du)$, which reduces to roughly $(du)^{-1/2} \cos(\pi du)$ for large arguments.

Within the above hypotheses, we infer that the ring diameter d should not change in time near the black hole. However, as we have shown in the previous sections, the expansion of the Universe makes d a time-dependent quantity, with a redshift drift similar to Eq. (13). Therefore, the ring diameter acquires in this picture a time dependence

$$\frac{\dot{d}}{d} = H_0 - \frac{H(z)}{1+z}, \quad (19)$$

and the relative variation of the visibility amplitude varies as

$$\begin{aligned} \frac{\dot{V}}{V} &= -\pi u \dot{d} \frac{J_1(\pi du)}{J_0(\pi du)} \\ &\simeq -\frac{1}{2} (\pi u d)^2 \frac{\dot{d}}{d} \\ &\simeq -\frac{1}{2} (\pi u d)^2 \left(H_0 - \frac{H(z)}{1+z} \right), \end{aligned} \quad (20)$$

where we have used the Bessel expansion for large argument $J_1(x)/J_0(x) \simeq x/2$ in the second line. This expansion is justified since the first photon ring should be resolved for large baselines, which implies $du \gg 1$. The visibility variation interestingly depends on u^2 , meaning that a greater baseline should probe a greater variation, as shown in Fig. 3. The effect is once again very small, with a best case of a variation about 10^{-6} per year for $z \simeq 0.5$ using a baseline $u = 10 \mu\text{as}^{-1}$, which would be barely attainable with a Moon-Earth array (see Fig. 5 in [43]). It is worthwhile though to mention that spectroscopic measurements are usually more precise than optical ones. It is expected that forthcoming surveys in the next few years will be able to detect a shift in the spectral lines of the order of $10^{-9} - 10^{-10}$ within an observational window of $\sim 10 \text{yr}$, see for example Ref. [4]. Therefore, if a similar precision can be reached for interferometric observations of photon rings, the task of measuring their drift does not seem hopeless.

A second interesting point is that the period also suffers from the redshift drift, with a relative change

$$\frac{\dot{\Delta u}}{\Delta u} = -\frac{\dot{d}}{d} = -\left(H_0 - \frac{H(z)}{1+z} \right), \quad (21)$$

opposite to the drift in the ring diameter. Since the $2/d$ periodicity is unlikely to be contaminated by other sources of emission on great baselines, the period is a universal signature which can be used to detect a black hole photon ring via the observed visibility. As an immediate consequence following from Eq. (21), the universal interferometric pattern should also change with time, along with the strength of the visibility amplitude.

⁴ Note that superradiance could potentially change the apparent angular diameter of the shadow [55, 56], and drift effects could have interesting applications for these models as well.

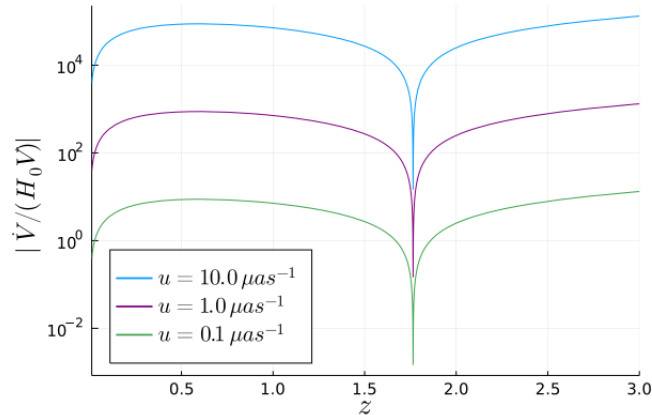


FIGURE 3. Variation of the visibility amplitude for a photon ring with apparent angular diameter $d = 40 \mu\text{as}$. The variation is a function of the redshift and drawn for three baselines ($u = 10, 1$, and $0.1 \mu\text{as}^{-1}$, in blue, purple and green, respectively). For a redshift $z = 0.004$ (M87*), the respective variations of the normalised amplitude $|\dot{V}/(H_0 V)|$ are of about 1.6×10^3 , 16.0 and 0.16 for each baseline, resulting in a change of the amplitude $|\dot{V}/V|$ of about a factor 3×10^{-11} , 3×10^{-13} and 3×10^{-15} per day.

5. CONCLUSIONS AND DISCUSSION

The main purpose of this work was to quantify the impact of cosmological drift on three important black hole physics observables: the black hole shadow's apparent angular diameter, the visibility, and the frequency (or equivalently the period) of its photon rings. The apparent angular diameter of the shadow, for a spherically symmetric black hole, is determined by its total mass M and the angular diameter distance D_A , which makes it a possible candidate standard ruler, see Refs. [61]. Similarly, the visibility amplitude and frequency inferred from interferometric universal signatures of photon rings are mostly determined by the ring diameter, which could potentially be a source of cosmological information, as discussed in Ref. [43]. The drifts of these three quantities are given by Eqs. (13), (19) and (21), respectively. In Fig. 1, the shadow drift is reported in units of H_0 up to redshift $z = 5$ assuming a fiducial Λ CDM cosmology with $\Omega_m = 0.33$ and $\Omega_\Lambda = 0.67$. At low redshift, $z \ll 1$, the maximum drift is of order $10^{-1} H_0$. For M87*, located at redshift $z \approx 4 \times 10^{-3}$, this results in a shadow drift of the order of $10^{-16} \text{ day}^{-1}$, which is beyond the angular resolution of the EHT and forthcoming experiments. Concerning the status of photon ring observations, current experiments do not have enough sensitivity to resolve individual rings. On the other hand, as discussed in Ref. [43], future Earth-Moon and Earth-L2 baselines will have enough precision to resolve the rings and allow for spectroscopic observations. In Fig. 3, the visibility amplitude drift is shown for three future experiments with baselines larger than the one currently in use with the EHT (which tops at $0.05 \mu\text{as}^{-1}$). The shift induced in the spectral lines by the Hubble flow is the most promising candidate to detect redshift drift effects and, as discussed in Ref. [4], can reach a precision of order 10^{-9} over a time span of a decade. If, in the future, such a precision can be reached for spectroscopic measurements of photon rings, observing their visibility amplitudes and frequencies drifts does not seem hopeless.

It is interesting to note that the formula for the black hole shadow (13) is very similar to the one obtained for the lens equation in the thin-lens approximation, being proportional to the product of the Newton constant and the object mass $G_N M$ and inversely proportional to the angular diameter distance. In the same fashion as what has been done for strong lensing observables [17], it is possible to translate non-observations of drift effects within the sensitivity of current experiments into a constraint on the violation of the Equivalence Principle in theories featuring a time-dependent gravitational coupling G_{eff} . We quantified the non-observations of a drift in the size of M87*'s shadow over a period of one year, within the current sensitivity of EHT, into a constraint on $\dot{G}_{eff}/G_{eff} \leq 10^{-4}$. This constraint, however, is obtained assuming that the mass of the black hole M does not vary with time. On the other hand, if this is the case, variations of the black hole shadow within the framework of General Relativity can be used to verify accretion models of black holes. Using the current sensitivity of EHT, the non-observations of a shadow drift over a period of one year gives a constraint on the variation of M87*'s mass of $\Delta M \leq 10^5 M_\odot$.

While most of the effects we presented in this paper are beyond the sensitivity of current experiments, it is worthwhile to recognize and quantify the amount of cosmological information encoded within black hole shadows for future long-monitoring programs. Furthermore, these observations have the potential to become an important test of the equivalence principle in a strong gravity regime, thus complementing other existing probes.

In this work, we considered variations in the shadow of a single, spherically symmetric Black hole embedded in a FLRW Universe. It would also be very interesting to study how the results we obtained change when we relax these assumptions. As was discussed in [62], the shadow of a Kerr black hole can be obtained in a similar way as for a McVittie black hole, which we used in this paper. The shadow obtained by these authors is quite similar to those in McVittie, with two different angular sizes due to the black hole spin. By reproducing the steps of our paper to this Kerr-de Sitter framework, we obtain the same qualitative results. However, the embedding of a Kerr black hole into a FLRW background is not unique, as the former breaks not only homogeneity of the spacetime (like in McVittie) but also isotropy, introducing dragging effects relative to the rotation axes which makes the results observer dependent.

To conclude, we mention that it would be very interesting to study the time dependence of the shadow(s) profile(s) for two or more interacting black holes [63]. Indeed, in this case one expects that the mass loss due to the production of gravitational waves (GW) should correspond to a shrinking of the shadow(s). However, it must be stressed that the GW signal during the inspiral

phase depends on a particular combination of the black hole masses, *i.e.* the chirp mass, whose relation with the diameter of the shadow(s) is not trivial. Furthermore, the GW response function is affected in a similar way by the cosmological expansion, by a time-dependent gravitational coupling and by a time-varying mass [64]. As a result, if one tries to relate the GW signal with a drift of the shadow(s), these effects will all be degenerate in the final measurement. We believe that these directions deserve further investigations, which we leave for future works.

ACKNOWLEDGMENTS

We are grateful to Tamara Davis, Oliver Piattella, and Sunny Vagnozzi for valuable comments and discussions. EF thanks the Helsinki Institute of Physics for its warm hospitality. LG acknowledges support from the Australian Government through the Australian Research Council Laureate Fellowship grant FL180100168.

REFERENCES

- [1] A. Sandage, *The change of redshift and apparent luminosity of galaxies due to the deceleration of selected expanding universes.*, *The Astrophysical Journal* **136** (1962) 319.
- [2] G. C. McVittie, *Appendix to the change of redshift and apparent luminosity of galaxies due to the deceleration of selected expanding universes.*, *The Astrophysical Journal* **136** (1962) 334.
- [3] E. V. Linder, *Constraining models of dark energy*, [1004.4646](#).
- [4] A. G. Kim, E. V. Linder, J. Edelman and D. Erskine, *Giving Cosmic Redshift Drift a Whirl*, *Astropart. Phys.* **62** (2015) 195–205, [[1402.6614](#)].
- [5] F. A. Teppa Pannia and S. E. Perez Bergliaffa, *Constraining $f(R)$ theories with cosmography*, *JCAP* **08** (2013) 030, [[1301.6140](#)].
- [6] P. Mishra and M.-N. C el erier, *Redshift and redshift-drift in $\Lambda = 0$ quasi-spherical Szekeres cosmological models and the effect of averaging*, [1403.5229](#).
- [7] C. J. A. P. Martins, M. Martinelli, E. Calabrese and M. P. L. P. Ramos, *Real-time cosmography with redshift derivatives*, *Phys. Rev. D* **94** (2016) 043001, [[1606.07261](#)].
- [8] S. Pandolfi and M. Martinelli, *Probing dark energy with redshift drift*, *Proc. Int. Sch. Phys. Fermi* **186** (2014) 327–333.
- [9] C. S. Alves, A. C. O. Leite, C. J. A. P. Martins, J. G. B. Matos and T. A. Silva, *Forecasts of redshift drift constraints on cosmological parameters*, *Mon. Not. Roy. Astron. Soc.* **488** (2019) 3607–3624, [[1907.05151](#)].
- [10] H.-R. Kl ockner, D. Obreschkow, C. Martins, A. Raccanelli, D. Champion, A. L. Roy et al., *Real time cosmology - A direct measure of the expansion rate of the Universe with the SKA*, *PoS AASKA14* (2015) 027, [[1501.03822](#)].
- [11] O. F. Piattella and L. Giani, *Redshift drift of gravitational lensing*, *Phys. Rev. D* **95** (2017) 101301, [[1703.05142](#)].
- [12] F. Melia, *Definitive test of the $R_h = ct$ universe using redshift drift*, *Mon. Not. Roy. Astron. Soc.* **463** (2016) L61–L63, [[1608.00047](#)].
- [13] F. A. Teppa Pannia, S. E. Perez Bergliaffa and N. Manske, *Cosmography and the redshift drift in Palatini $f(R)$ theories*, *Eur. Phys. J. C* **79** (2019) 267, [[1811.08176](#)].
- [14] K. Bolejko, C. Wang and G. F. Lewis, *Direct detection of the cosmic expansion: the redshift drift and the flux drift*, [1907.04495](#).
- [15] M. Martinelli, S. Pandolfi, C. J. A. P. Martins and P. E. Vielzeuf, *Probing dark energy with the Sandage-Loeb test*, *Phys. Rev. D* **86** (2012) 123001, [[1210.7166](#)].
- [16] M. Quartin and L. Amendola, *Distinguishing Between Void Models and Dark Energy with Cosmic Parallax and Redshift Drift*, *Phys. Rev. D* **81** (2010) 043522, [[0909.4954](#)].
- [17] L. Giani and E. Frion, *Testing the Equivalence Principle with Strong Lensing Time Delay Variations*, *JCAP* **09** (2020) 008, [[2005.07533](#)].
- [18] R. Codur and C. Marinoni, *Redshift drift in radially inhomogeneous Lem atre-Tolman-Bondi spacetimes*, [2107.04868](#).
- [19] EVENT HORIZON TELESCOPE collaboration, K. Akiyama et al., *First M87 Event Horizon Telescope Results. IV. Imaging the Central Supermassive Black Hole*, *Astrophys. J. Lett.* **875** (2019) L4, [[1906.11241](#)].
- [20] EVENT HORIZON TELESCOPE collaboration, K. Akiyama et al., *First M87 Event Horizon Telescope Results. II. Array and Instrumentation*, *Astrophys. J. Lett.* **875** (2019) L2, [[1906.11239](#)].
- [21] EVENT HORIZON TELESCOPE collaboration, K. Akiyama et al., *First M87 Event Horizon Telescope Results. I. The Shadow of the Supermassive Black Hole*, *Astrophys. J. Lett.* **875** (2019) L1, [[1906.11238](#)].
- [22] EVENT HORIZON TELESCOPE collaboration, K. Akiyama et al., *First M87 Event Horizon Telescope Results. VI. The Shadow and Mass of the Central Black Hole*, *Astrophys. J. Lett.* **875** (2019) L6, [[1906.11243](#)].
- [23] EVENT HORIZON TELESCOPE collaboration, K. Akiyama et al., *First M87 Event Horizon Telescope Results. V. Physical Origin of the Asymmetric Ring*, *Astrophys. J. Lett.* **875** (2019) L5, [[1906.11242](#)].
- [24] EVENT HORIZON TELESCOPE collaboration, K. Akiyama et al., *First M87 Event Horizon Telescope Results. III. Data Processing and Calibration*, *Astrophys. J. Lett.* **875** (2019) L3, [[1906.11240](#)].
- [25] EVENT HORIZON TELESCOPE collaboration, K. Akiyama et al., *First M87 Event Horizon Telescope Results. VII. Polarization of the Ring*, *Astrophys. J. Lett.* **910** (2021) L12, [[2105.01169](#)].
- [26] J. M. Bardeen, *Timelike and null geodesics in the Kerr metric*, in *Les Houches Summer School of Theoretical Physics: Black Holes*, 1973.
- [27] C. Bambi, K. Freese, S. Vagnozzi and L. Visinelli, *Testing the rotational nature of the supermassive object M87* from the circularity and size of its first image*, *Phys. Rev. D* **100** (2019) 044057, [[1904.12983](#)].
- [28] A. Allahyari, M. Khodadi, S. Vagnozzi and D. F. Mota, *Magnetically charged black holes from non-linear electrodynamics and the Event Horizon Telescope*, *JCAP* **02** (2020) 003, [[1912.08231](#)].
- [29] S. Hadar, M. D. Johnson, A. Lupsasca and G. N. Wong, *Photon Ring Autocorrelations*, *Phys. Rev. D* **103** (2021) 104038, [[2010.03683](#)].
- [30] E. Himwich, M. D. Johnson, A. Lupsasca and A. Strominger, *Universal polarimetric signatures of the black hole photon ring*, *Phys. Rev. D* **101** (2020) 084020, [[2001.08750](#)].
- [31] S. G. Ghosh, R. Kumar and S. U. Islam, *Parameters estimation and strong gravitational lensing of nonsingular Kerr-Sen black holes*, *JCAP* **03** (2021) 056, [[2011.08023](#)].
- [32] M. Afrin, R. Kumar and S. G. Ghosh, *Parameter estimation of hairy Kerr black holes from its shadow and constraints from M87**, *Mon. Not. Roy. Astron. Soc.* **504** (2021) 5927–5940, [[2103.11417](#)].
- [33] A. E. Broderick, P. Tiede, D. W. Pesce and R. Gold, *Measuring Spin from Relative Photon Ring Sizes*, [2105.09962](#).
- [34] F. Roelofs, C. M. Fromm, Y. Mizuno, J. Davelaar, M. Janssen, Z. Younsi et al., *Black hole parameter estimation with synthetic Very Long Baseline Interferometry data from the ground and from space*, *Astron. Astrophys.* **650** (2021) A56, [[2103.16736](#)].
- [35] S. Vagnozzi and L. Visinelli, *Hunting for extra dimensions in the shadow of M87**, *Phys. Rev. D* **100** (2019) 024020, [[1905.12421](#)].
- [36] M. Khodadi, A. Allahyari, S. Vagnozzi and D. F. Mota, *Black holes with scalar hair in light of the Event Horizon Telescope*, *JCAP* **09** (2020) 026, [[2005.05992](#)].
- [37] S. E. Gralla, A. Lupsasca and D. P. Marrone, *The shape of the black hole photon ring: A precise test of strong-field general relativity*, *Phys. Rev. D* **102** (2020) 124004, [[2008.03879](#)].
- [38] EVENT HORIZON TELESCOPE collaboration, D. Psaltis et al., *Gravitational Test Beyond the First Post-Newtonian Order with the Shadow of the M87 Black Hole*, *Phys. Rev. Lett.* **125** (2020) 141104, [[2010.01055](#)].
- [39] C. Li, H. Zhao and Y.-F. Cai, *New test on the Einstein equivalence principle through the photon ring of black holes*, [2102.10888](#).
- [40] F. Aratore and V. Bozza, *Decoding a black hole metric from the interferometric pattern of relativistic images*, [2107.05723](#).
- [41] J.-Z. Qi and X. Zhang, *A new cosmological probe using super-massive black hole shadows*, *Chin. Phys. C* **44** (2020) 055101, [[1906.10825](#)].
- [42] V. Perlick and O. Y. Tsupko, *Calculating black hole shadows: review of analytical studies*, [2105.07101](#).
- [43] M. D. Johnson et al., *Universal interferometric signatures of a black hole’s photon ring*, *Sci. Adv.* **6** (2020) eaaz1310, [[1907.04329](#)].
- [44] S. E. Gralla, *Measuring the shape of a black hole photon ring*, *Phys. Rev. D* **102** (2020) 044017, [[2005.03856](#)].
- [45] G. C. McVittie, *The mass-particle in an expanding universe*, *Mon. Not. Roy. Astron. Soc.* **93** (1933) 325–339.
- [46] O. Y. Tsupko and G. S. Bisnovatyi-Kogan, *First analytical calculation of black hole shadow in McVittie metric*, *Int. J. Mod. Phys. D* **29** (2020) 2050062, [[1912.07495](#)].
- [47] E. V. Linder, *First Principles of Cosmology*. 1997.
- [48] O. F. Piattella, *Lensing in the McVittie metric*, *Phys. Rev. D* **93** (2016) 024020, [[1508.04763](#)].

- [49]S. Vagnozzi, C. Bambi and L. Visinelli, *Concerns regarding the use of black hole shadows as standard rulers*, *Class. Quant. Grav.* **37** (2020) 087001, [2001.02986].
- [50]M. Cappellari, E. Emsellem, D. Krajnović, R. M. McDermid, N. Scott, G. Verdoes Kleijn et al., *The atlas3d project—i. a volume-limited sample of 260 nearby early-type galaxies: science goals and selection criteria*, *Monthly Notices of the Royal Astronomical Society* **413** (2011) 813–836, [1012.1551].
- [51]T. Lisker, R. Vijayaraghavan, J. Janz, J. S. Gallagher III, C. Engler and L. Urich, *The active assembly of the virgo cluster: Indications for recent group infall from early-type dwarf galaxies*, *The Astrophysical Journal* **865** (2018) 40, [1808.04751].
- [52]S.-F. Yan, C. Li, L. Xue, X. Ren, Y.-F. Cai, D. A. Easson et al., *Testing the equivalence principle via the shadow of black holes*, *Phys. Rev. Res.* **2** (2020) 023164, [1912.12629].
- [53]G. Alestas, I. Antoniou and L. Perivolaropoulos, *Hints for a gravitational constant transition in Tully-Fisher data*, **2104.14481**.
- [54]L.-X. Li, *Accretion, Growth of Supermassive Black Holes, and Feedback in Galaxy Mergers*, *Mon. Not. Roy. Astron. Soc.* **424** (2012) 1461, [1205.0363].
- [55]R. Roy and U. A. Yajnik, *Evolution of black hole shadow in the presence of ultralight bosons*, *Phys. Lett. B* **803** (2020) 135284, [1906.03190].
- [56]G. Creci, S. Vandoren and H. Witek, *Evolution of black hole shadows from superradiance*, *Phys. Rev. D* **101** (2020) 124051, [2004.05178].
- [57]R. Brito, V. Cardoso and P. Pani, *Black holes as particle detectors: evolution of superradiant instabilities*, *Class. Quant. Grav.* **32** (2015) 134001, [1411.0686].
- [58]E. Barausse, V. Cardoso and P. Pani, *Can environmental effects spoil precision gravitational-wave astrophysics?*, *Phys. Rev. D* **89** (2014) 104059, [1404.7149].
- [59]W. Forman, E. Churazov, C. Jones, S. Heinz, R. Kraft and A. Vikhlinin, *Partitioning the Outburst Energy of a Low Eddington Accretion Rate AGN at the Center of an Elliptical Galaxy: the Recent 12 Myr History of the Supermassive Black Hole in M87*, *Astrophys. J.* **844** (2017) 122, [1705.01104].
- [60]S. E. Gralla, D. E. Holz and R. M. Wald, *Black Hole Shadows, Photon Rings, and Lensing Rings*, *Phys. Rev. D* **100** (2019) 024018, [1906.00873].
- [61]O. Y. Tsupko, Z. Fan and G. S. Bisnovatyi-Kogan, *Black hole shadow as a standard ruler in cosmology*, *Class. Quant. Grav.* **37** (2020) 065016, [1905.10509].
- [62]P.-C. Li, M. Guo and B. Chen, *Shadow of a Spinning Black Hole in an Expanding Universe*, *Phys. Rev. D* **101** (2020) 084041, [2001.04231].
- [63]A. Yumoto, D. Nitta, T. Chiba and N. Sugiyama, *Shadows of Multi-Black Holes: Analytic Exploration*, *Phys. Rev. D* **86** (2012) 103001, [1208.0635].
- [64]N. Yunes, F. Pretorius and D. Spergel, *Constraining the evolutionary history of Newton's constant with gravitational wave observations*, *Phys. Rev. D* **81** (2010) 064018, [0912.2724].